

Research Article

Optimal Design of Sports Event Timer Structure Based on Ferroelectric Memory

Jiannan Liu ¹ and Cailie Chen ²

¹Sport Department, Chongqing Jiaotong University, Chongqing 400074, China

²College of Mechanical and Vehicle Engineering, Chongqing University, Chongqing 400000, China

Correspondence should be addressed to Cailie Chen; chencailie@cqu.edu.cn

Received 3 March 2022; Revised 7 May 2022; Accepted 24 May 2022; Published 15 June 2022

Academic Editor: Awais Ahmed

Copyright © 2022 Jiannan Liu and Cailie Chen. This is an open access article distributed under the Creative Commons Attribution License, which permits unrestricted use, distribution, and reproduction in any medium, provided the original work is properly cited.

Sports events are an indispensable part of popularization and strong entertainment and can promote the physical and mental health of the people and the construction of cultural and spiritual civilization. Therefore, it is necessary to use a timer to record and analyze data during the game. In the traditional sense, the game timer is a fixed system. And now we can design sports event timer operations through mobile phones, computers, and other equipment to assist in the calculation of game time and competition. Ferroelectric memory is a kind of random access memory, which combines the fast read and write access of dynamic random access memory with the ability to retain data. Based on this, the ferroelectric memory timer proposed in this paper is intended to improve the accuracy and fairness of sports events. Therefore, this article has tested the function of the timer designed in this article by studying the ferroelectric memory and experimental construction and testing methods and finally concluded that the design is reasonable, but there is still a problem of data susceptibility. The experimental results show that there is a certain gap between the time interval measurement level of the timer and SR, the difference is 47 ps, the pulse width difference is controlled at 0.004, and the measurement uncertainty of timer interval is better than 60 ps. This shows that the timer can be applied, but it needs further improvement.

1. Introduction

Ferroelectric memory has the characteristics of small size and low power consumption. It has a wide frequency range used in sports competitions, mainly used for timing sports events, and can also be used as other equipment such as stylus pens and other physical sports counting tools. Its internal structure is relatively simple, the volume is relatively small, the performance is stable, and the anti-interference ability is very good. Large storage space, small size, and light weight are one of the main characteristics of ferromagnetic materials. This feature is also closely related to the application value: when used in sports timers, it can not only realize the data storage function but also effectively improve the efficiency of the game.

The sports event timer is a device that can record the time of the event. It consists of a display screen, buttons, and a timer. Count according to the time of the sporting

event and display it on the display screen, so that you can visually see all the data recorded on the display. This not only improves work efficiency but also avoids erroneous actions. Specifically, it releases the clock information in real-time and accurately through the front-end multiseed clock equipment, so that the time of each intelligent system is centralized and synchronized. After the game is over, the statistics and analysis of the data in the game timer are also a technical method [1]. In order to achieve the structural optimization design of the sports game timer, it is necessary to implement its technical indicators on the software.

When the traditional timer is used for sports competitions, the data to be displayed is usually first input to the display and then displayed on the display. Although this has the advantages of intuitiveness and convenient operation. But to a certain extent, it will give people a feeling of cumbersome, inconvenient, and error-prone. So there are many researches on sports timers and ferroelectric memory. Memory allows

designers to write data to nonvolatile memory faster and more frequently at a lower price [2]. Among them, Li et al. took the FM28V100 ferroelectric memory model as the research object, conducted electron radiation experiments, and studied the damage law of the total radiation dose of the ferroelectric memory under different working methods and different radiation sources [3]. An'an et al. conducted an experimental study on the single-event effects of medium and high energy protons on two commercial ferroelectric memories and found that one of the devices exhibited single-event reversal and functional interruption under proton irradiation [4]. Feizhuan et al.'s traditional basketball game uses manual scoring or flops and uses a timer to complete the game timing. This timing and scoring involve many human factors, which affect the fairness of the game and the fairness of performance to a certain extent [5]. Pengcheng combined the NBA game rules and put forward a 24-second countdown overall plan for basketball games based on the AHDL language [6]. In order to overcome the shortcomings of existing microcontroller timer applications that cannot be paused or restarted, Kang describes a timer that uses external interrupts to pause or restart [7]. Xiaocheng et al. proposed the design requirements of basketball timers according to FIBA's requirements for the DE10_Lite timer and functions of Uniview Technology [8]. In sports events, the accuracy of the timer is a symbol of fairness in the arena. The ferroelectric memory has the characteristics of less interference, so it is a way of choice to apply it to the timer.

The innovation of this paper is to compare the advantages between them by studying the types of ferroelectric memory, ferroelectric film capacitors, ferroelectric storage technology, and structure and functional principles, then propose a sports timer based on ferroelectric memory, and carry out this system structure design and analysis. Through analysis and design and further experimental verification, the designed timers are compared in terms of pulse width and time accuracy. Thereby, the experimental data results and conclusions can be drawn.

2. The Structure Timer of Sports Event Timer Based on Ferroelectric Memory

2.1. Ferroelectric Memory

2.1.1. Classification of Ferroelectrics. Ferroelectric crystals include gallium arsenide, lamination, multijunction, and perovskite. Among all ferroelectric crystals, the perovskite structure is the most typical and common structure. Although it was later discovered that CaTiO₃ is actually a twisted perovskite structure, the name still exists [9, 10].

2.1.2. Ferroelectric Film Capacitor. Ferroelectric film capacitors are a type of flat capacitors. Using the knowledge of dielectric physics, we know that the charge H stored in a capacitor can be expressed as

$$H = S \cdot C. \quad (1)$$

Among them, S is the area of the capacitor plate, and C is

the electric displacement vector in the ferroelectric film. The definition of electric displacement vector is

$$C = M(F) + \theta_0 F, \quad (2)$$

where F is the electric field strength (physical quantity indicating the strength and direction of electric field), and the θ_0 is dielectric constant. M is the polarization intensity, which is a nonlinear function of F . The electric field strength F can be expressed as

$$F = \frac{v}{t}, \quad (3)$$

where v is the voltage and t is the thickness of the ferroelectric film. The polarization intensity M can be expressed as

$$M(F) = \theta_0 (\theta_q(F) - 1) \cdot F. \quad (4)$$

θ_q is the relative permittivity, which is also a function of the electric field F . Substituting formula (1) into formula (2) and taking into account that the relative permittivity of ferroelectrics is usually much greater than that, we can get

$$C(F) = \theta_0 \cdot \theta_q(F) \cdot F \approx \theta_0 \cdot (\theta_q(F) - 1) \cdot F = M. \quad (5)$$

Substituting this approximate expression into equation (1), we can get

$$P = G_{\text{dip}} + G_F + G_g. \quad (6)$$

Formula (6) relates the microscopic physical quantity in the ferroelectric film to the macroscopic measurable charge quantity. Iron sheet structure film is composed of several grains with different sizes. The total free energy P of the polycrystalline film is composed of three parts. The surface depolarization field does work G_F , the domain wall pinning field does work G_g , and the dipole flips work G_{dip} , namely,

$$P = G_{\text{dip}} + G_F + G_g. \quad (7)$$

If the film is very thin and can only accommodate one layer of electrical domains, the polarization direction of the ferroelectric domains is perpendicular to the electrode and the orientation is the same, then:

$$F = -\frac{1}{\theta_0} M. \quad (8)$$

If the situation is a little more complicated, the polarization direction of the domains perpendicular to the interface will periodically change, and this distribution makes G_{dip} reach the minimum value. At this time, there are

$$G_F = \frac{\theta^* \cdot k \cdot M_0 \cdot v}{t}. \quad (9)$$

Among them, t is the thickness of the film, k is the width of the electric domain, M_0 is the polarization intensity in each electric domain, v is the volume of the entire film, and θ^* is a factor related to the dielectric constant. If the rolling work μ_{wall} is determined per unit area of the domain wall, the total work G_g done by the domain wall is

$$G_g = \frac{\mu_{\text{wall}}}{k} \cdot v. \quad (10)$$

Combining formulas (9) and (10), there are

$$G_F + G_g = \frac{\theta^* \cdot k \cdot M_0 \cdot v}{t} + \frac{\mu_{\text{wall}}}{k} \cdot v. \quad (11)$$

When formula (11) takes the minimum value, there are

$$k = \sqrt{\frac{\mu_{\text{wall}} \cdot t}{\theta^* \cdot M_0^2}}. \quad (12)$$

From formula (12), the following conclusion can be drawn: as long as the polarization of the ferroelectric thin film is not zero, the ferroelectric domain width is a finite domain wall. Neither work nor domain width k will be 0 [11, 12].

2.1.3. The Structure and Function Principle of Ferroelectric Memory. The function of storing data in ferroelectric memory is mainly completed by ferroelectric capacitors with thin-film ferroelectric materials as the carrier [13]. Generally speaking, ferroelectric materials do not contain “iron,” but refer to ferroelectric crystals. Compared with traditional nonvolatile memory such as EEPROM and FLASH, ferroelectric memory has lower leakage current, because the data storage of ferroelectric memory is not carried out by free electrons, but by atomic polarization [14, 15]. When an electric field is applied to a ferroelectric crystal, the central atom inside the ferroelectric crystal will move and change with the distribution of the electric field. When the atom gains a certain amount of energy, the violent movement of free carriers in the crystal expands rapidly, causing the charge to collapse [16]. In this case, the polarization of the ferroelectric material is a certain function of the applied electric field. When the applied electric field disappears, the polarization of the ferroelectric material becomes stable, and the corresponding data information is stored in the ferroelectric crystal [17, 18].

Figure 1 shows the hysteresis loop block diagram of the ferroelectric capacitor and the block diagram of the ferroelectric memory. In (1), the abscissa represents the applied electric field, and the ordinate represents the polarization intensity. Figure (a) is a schematic diagram of 1T1C ferroelectric memory. Among them, the word line is connected to the gate of the transistor to control the turn-on and turn-off of the transistor. The bit line is connected to the source of the transistor. Figure (b) is a block diagram of 1T2C ferroelectric memory, the structure is similar to 1T1C ferroelectric memory [19, 20].

The manufacturing technology of ferroelectric memory integrates ferroelectric thin film process and traditional CMOS process. Ferroelectric memory not only includes a ferroelectric memory array that stores data but also includes CMOS peripheral circuits that amplify and read signals, control timing signals, and data latch functions [21, 22].

FRAM has many advantages and is suitable for embedded systems. It is a new type of memory with relatively mature industrialization technology. It can work in extreme environments and may replace Si-based devices that currently require heat preservation devices to be used in spacecraft or aerospace probes. In order to reduce launch costs or increase satellite functions, it is considered to have great potential for space applications. Compared with SRAM, although ferroelectric memory is not advantageous in terms of speed and price, from the perspective of the overall design, ferroelectric memory still has certain advantages. Ferroelectric memory is very resistant to electromagnetic radiation, elementary particle radiation, and nuclear radiation. They generally will not interfere with the stored information due to the radiation of a single charged particle, and they can withstand high dose rates of X-rays and neutrons and large total doses of radiation [23].

2.2. Sports Event Timer Based on Ferroelectric Memory. The sports event timer based on ferroelectric memory is mainly composed of two parts: hardware circuit and software program. A simple circuit diagram is designed in the hardware part. First use a multimeter to measure whether the connection between each device and the microcontroller is correct. Then through the analysis of the data, the corresponding parameter values are obtained and displayed. At the same time, these variables can be converted into voltage signals and input to the PC terminal.

The sports event timer based on ferroelectric memory uses the digital pulse waveform to convert the data into the required signal through the analog circuit and then process it by the single-chip microcomputer. The output of the analog circuit is a sine wave, variance, time interval, and other parameter information; and in actual use, due to some uncertain factors that affect the final result, it will lead to large errors or inaccurate realization of moving objects within the measurement value range. And so on, digital integrated circuits can be used to complete data acquisition and control.

The working principle of ferroelectric memory is first, in the display, there is a sliding rheostat and two data drive boards. When a certain number appears on the display screen (red LED red light). Then connect the data line to the intermediate relay control module for data recording and storage; finally, the corresponding time, location, and other information will be displayed on the display screen for people’s reference (including the time unit of sports events). The structure design of the ferroelectric memory mainly utilizes a sliding rheostat and two light-emitting diodes. The specific design is shown in Figure 2.

The game timer based on ferroelectric memory does not need to be modified in the program. First, it is simulated by software, and then, its function and implementation method

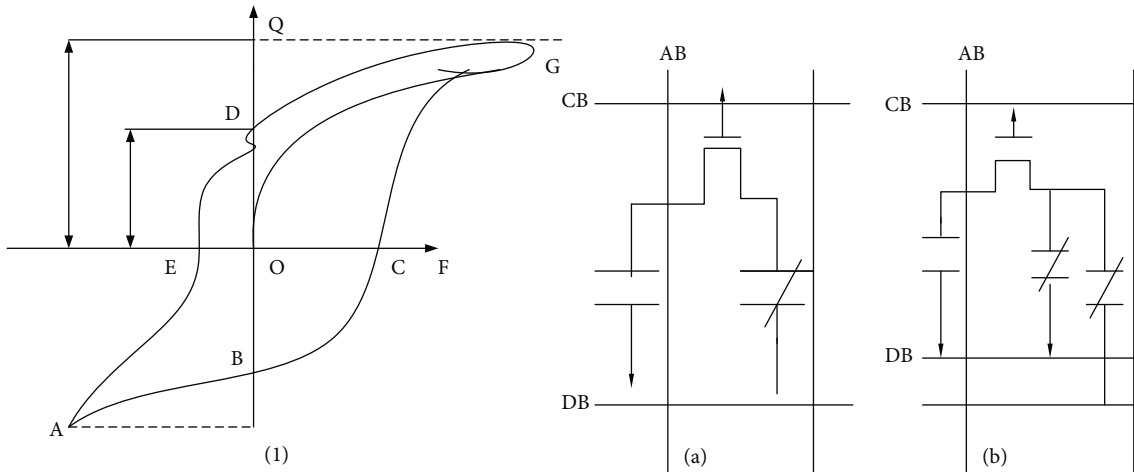


FIGURE 1: Electric circuit of ferrocapacitance and ferroelectric memory circuit structure.

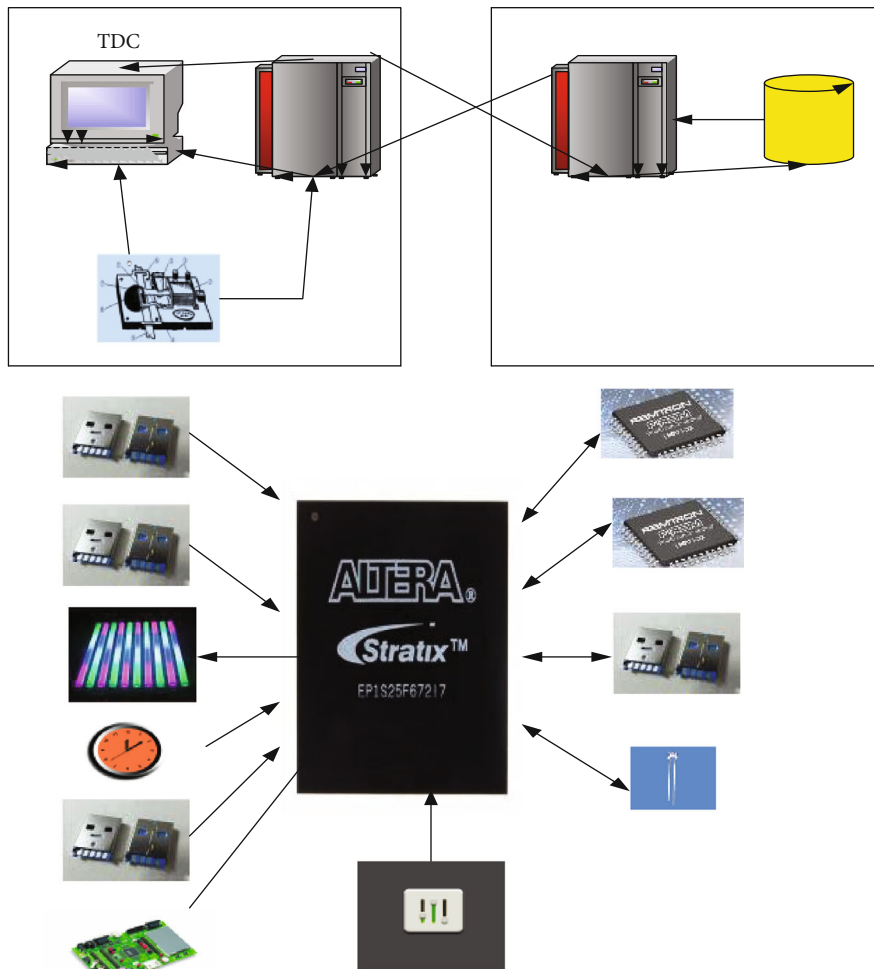


FIGURE 2: Functional block diagram of Stratix FPGA development board.

are improved. When used, the display was found to be the same as the previous design. However, because there are many interference factors in the hardware circuit that affect the display effect of the display screen and cannot save the

data content information well; second, the software part does not add the corresponding module so that it can better utilize the functions of the PC to complete the accuracy index required by timer (for example: time and speed).

2.3. Design of Two-Step Timer. The two-step TDC is actually not a fixed circuit structure, but a TDC design idea that combines two TDC basic structures. Usually, two structures with complementary advantages are selected for design in the basic implementation structure of TDC. In order to take into account the time resolution accuracy and dynamic range of this subject, while completing the layout design in the smallest possible area, a combination of pulse counting TDC and delay line-based TDC was selected. The two-step TDC combines the advantages of the basic clock cycle counting method and the delay line-based TDC two timing methods and can achieve both dynamic range and time resolution accuracy. The “two-step” of two-step TDC has a dual meaning. The first meaning is expressed in the structure of the TDC. The start signal and the stop signal, respectively, represent the timing start signal and timing end signal of the TDC. The two-step TDC has a two-stage structure, namely, the fine interpolator and the coarse timer. These two modules are also the two most critical modules of the two-step TDC. They have their own division of labor when measuring the time interval to be measured.

Choosing a suitable delay unit is very critical for realizing the ideal time resolution accuracy of TDC. The structures of delay units that are often used include inverters, buffers, differential inverters, and switching inverters. The inverter has the greatest advantages in terms of structure, time resolution accuracy, and area. Regarding the delay line structure, the design challenge is to ensure the linearity of the circuit. The inverter structure is single-ended input and single-ended output, which is more sensitive to noise. Using an inverter as a delay unit is bound to introduce fine interpolator greater nonideal factors. Therefore, considering the structure, time resolution accuracy, area, and antinoise ability, a differential inverter is used as the delay unit.

Based on the Cadence platform, the simulation of the fine timer is carried out. A rising edge signal is input to the fine timer during simulation, and the rising edge signal passes through the delay unit on the delay line. The position of the rising edge will lag equidistantly on the time axis, and the simulation results are consistent with the theoretical analysis. At the same time, it can be seen that after the input rising edge signal passes through the delay line, there is a delay, and the delay of each delay unit is about 186 ps. Therefore, the designed two-step TDC fine interpolator has a time resolution accuracy of 186 ps and a dynamic range of 2 ns.

The coarse adjustment timer is a circuit that can record the number of clock cycles of the reference clock, that is, the pulse timer. A binary timer can be used in the specific circuit design. The basic unit of a binary timer is an edge-type flip-flop. Among them, if you want to realize the function of clearing the output state of the coarse adjustment timer, the trigger needs to be improved.

The two-step TDC uses a coarse adjustment timer to process the time to be measured that is an integer multiple of the reference clock period, while the residual time uses a 16-bit fine interpolator for processing. Its timing error sources are the timer and the interpolator.

The work of the two key circuit modules of the two-step TDC—the fine interpolator and the coarse timer—is controlled by the edge signal. The signal propagates in the circuit and will inevitably be interfered by noise, parasitics, and other factors, which will cause the signal to be distorted. One of the most straightforward ways to optimize single-shot accuracy is to increase the frequency of the reference clock. Another way to improve the single input accuracy of TDC is to interpolate the residual time, where the residual time refers to the time less than one reference clock cycle, that is, the part of the time processed by the fine interpolator in the two-step TDC.

The overall block diagram and workflow of the hardware design are shown in Figure 3. The hardware of this system includes single-chip microcomputer MSP430F149 and its peripheral circuit parts (reset circuit and clock crystal oscillator), relay part, independent button part, display part, and drive circuit part. The whole circuit is controlled by the single-chip MSP430F149; the key control mode, time, and step are driven by ULN2803; and the corresponding data is displayed on the LCD12864 display.

Driven by the clock circuit, the single-chip microcomputer can run normally and stably, mainly because of the operation of the clock circuit, which helps each component of the single-chip microcomputer to perform its own work well. This kind of operation among them is automatic. The clock circuit uses pulse signals to satisfy the operation of the hardware part. In order to proceed with the work progress of the circuit from the initial state, it is necessary to make the core parts of the system in the initial state.

For the clock circuit, from the point of view of the microcontroller, the significance of the clock circuit is to provide a signal that the circuit system can perform stably, and this signal is timed. In order to achieve such a state, two parts are required, one part is that the other part of the crystal oscillator is a matching peripheral circuit, and the so-called timing time is the timing clock of the system. Time is the timing clock of the system. The clock circuit is an oscillator, which provides a beat to the single-chip microcomputer. The single-chip microcomputer must perform various operations under the control of this beat. Therefore, the single-chip microcomputer will not work normally without a clock circuit. The clock circuit itself does not control anything. The clock circuit helps the microcontroller to work in a stable state. The subsystem clock, auxiliary clock signal, and main clock signal provide signals for the MSP430F149 microcontroller. The subsystem clock provides services for some peripheral high-speed operating circuit modules, the auxiliary clock signal provides services for some peripheral low-speed operating circuits, and the main clock signal is a normal circuit module operating in a stable state.

3. System Testing and Analysis

After the system design is completed, it is necessary to build an experimental platform to evaluate the performance of the system. First, it introduces the experimental testing methods and evaluation indicators used in this article. Then select the

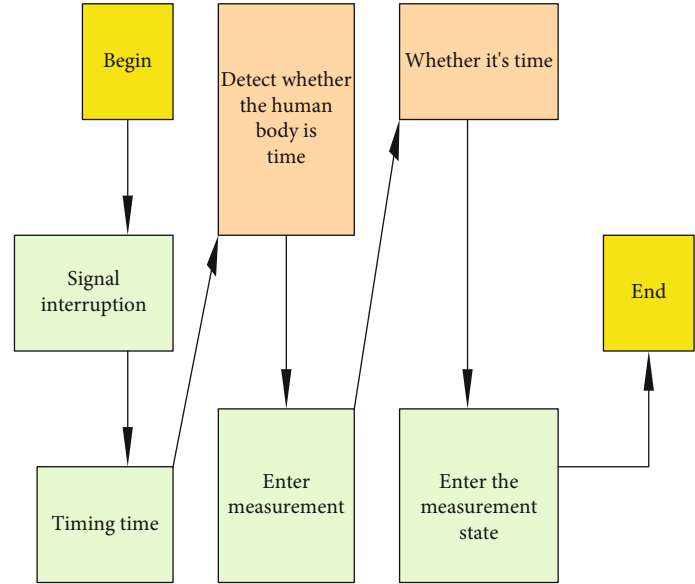
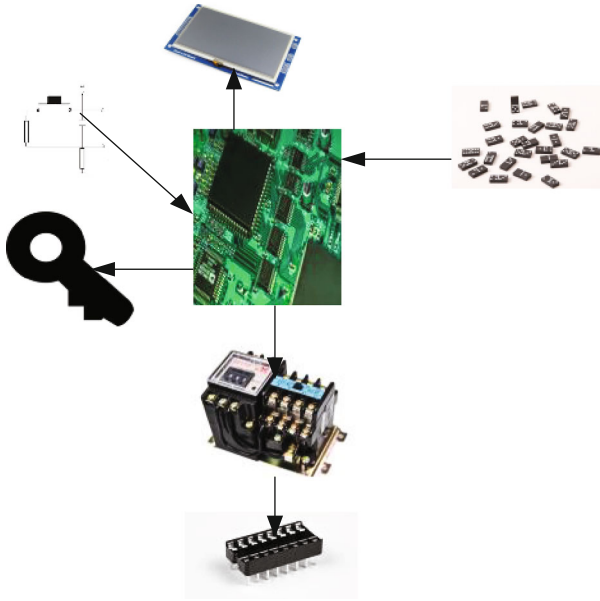


FIGURE 3: Overall block diagram and workflow of hardware design.

TABLE 1: Timer comparison with SR540 data results.

Time	Calculagraph	SR540	Time interval	Standard deviations
0	506.67	506.42	57.6/10.2	0.0562
1800	506.73	506.43	57.5/9.9	0.0573
3600	506.75	506.45	57.3/10.3	0.0596
5400	506.81	506.46	56.6/9.8	0.0654
7200	506.79	506.44	57.2/9.4	0.0725
9000	506.75	506.43	56.6/9.3	0.0849

signal source to test the accuracy of the timer's measurement. Finally, test the timer's time interval and pulse width measurement functions separately, use the test data to evaluate the performance indicators of the timer, and analyze the problems in the timer.

3.1. Test Method. The test platform with design specifications can make the test results more credible and provide a better reference for practical applications. In the field of time interval measurement, comparison method and fixed time interval measurement method are two commonly used test methods.

The comparison method is to use different measuring instruments to test the same signal source at the same time under the same external environment. The signal to be measured and the reference time are both generated by the same clock source and then transmitted to the measuring instrument through the same path, and the measurement is performed at the same time. This series of operations emphasizes the "same source." Then compare the measured results. In order to measure the performance of the developed measuring instrument, another instrument with very excellent performance is usually required. In this test platform, the measurement result of the SR540 time interval

timer with the best performance in the field of time measurement is selected as a reference for comparison.

The fixed time interval test method is to use the time interval measurement timer to measure the signal source to produce a fixed time interval without considering the cable and device delay. This method is simple to operate, and the result is more intuitive, but the signal quality of the signal source is very high. However, the accuracy of the time-to-digital conversion circuit is getting higher and higher, and the requirements for the signal source are getting higher and higher. At present, it is difficult to find a suitable signal source for testing in many cases. For this reason, this test platform does not design the realization of the fixed time interval test method separately but adopts the combination of the above two methods.

This platform uses the SR540-Timer universal time interval measurement device to compare with a channel of the timer, uses the 10 MHz signal generated by the National Time Service Center Clock Tower as the reference signal of the timer and the time base SR540, and then compares the time base of the 1 pps signal. The pulse distribution amplifier generates two signals to be measured, and each signal is sent through three channels and then sent from the other output terminal of the SR540 and the timer; the timer is connected to send the measurement results to the upper computer for processing. Different cable lengths can set different time intervals.

3.2. Evaluation Index. To design a measurement system, it is usually necessary to give the actual performance of the system, and scientific evaluation indicators are needed to evaluate the performance. In the field of time-frequency measurement, it is generally necessary to give the two indicators of system measurement deviation and measurement accuracy. Measurement deviation is usually affected by the stability of the time base, internal noise, trigger noise, and

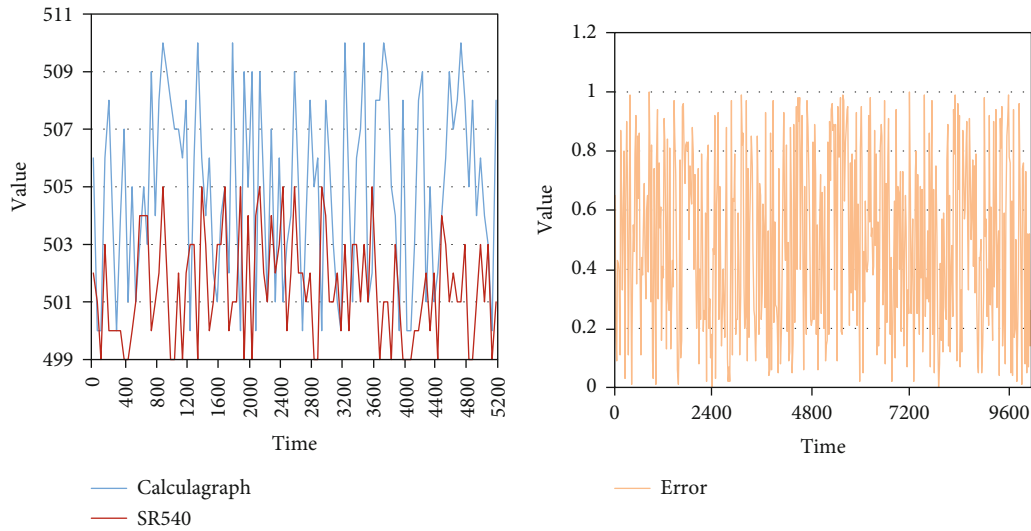


FIGURE 4: Alignment of timer and SR540 measurements and error plots.

TABLE 2: Timer and SR540 pulse width measurement contrast and error value.

Time	Calculagraph	SR540	Error
0	204.859	204.857	0.41
1000	204.857	204.856	0.45
2000	204.856	204.852	0.44
3000	204.86	204.854	0.56
4000	204.856	204.855	0.47
5000	204.854	204.853	0.45
6000	204.852	204.854	0.53
7000	204.853	204.856	0.46
8000	204.854	204.856	0.55
9000	204.855	204.857	0.5

uncertainty within the system. This concept is considered more when the “absolute” value of the measurement is more important. This paper uses the standard deviation of the experimental data to characterize the measurement accuracy of the system. This is because the designed test platform mainly uses the delay line test method, that is, two delay lines of different lengths and different delays are used to send the signal to be measured into the measurement. The channel is tested. Two different delay lines produce a fixed time interval, but the exact true value of this interval cannot be determined, so it is more appropriate to use the standard deviation as an evaluation index of measurement accuracy. The standard deviation is usually a statistic used to characterize the degree of dispersion of the system measurement value relative to the mean value.

3.3. System Test. First, analyze and evaluate the accuracy of the system measurement. Test the time interval measurement function of the timer. When measuring, the reference clock uses the 10 MHz frequency signal of the clock room of the National Time Service Center. The signal to be mea-

sured is 1 pps. The signal is delayed by a length of 100 m extension cable. The timer generally has 2-4 measurement channels, which will trigger sr540, so as to adjust the level to be consistent with the trigger level of this system.

Evaluate the accuracy of the system measurement. In the actual test, the measurement value of the SR540 can be regarded as the true value based on the test method of the comparison method, and the timer and the SR540 can be measured synchronously. Subtract the value of to get the difference between the two, which can be regarded as the accuracy of the system.

When measuring the pulse width, first, when configuring the chip, set the function to pulse width measurement, that is, configure the value of configuration register 1 to 2 f. In actual measurement, TDC-GPX2 internally connects measurement pins 1 and 3 (or 2 and 4) to an input pin (STOP1 or STOP2). The rising edge is measured by channel 1 (or 2), and the falling edge is measured by channel 3 (or 4). Then make the difference of the measurement result to get the value of pulse width.

4. Analysis of Test Results

4.1. Time Interval Measurement Performance Test. Calculate the measurement results and summarize the results with Table 1. The experimental value takes 2.5 hours of synchronized measurement results and then statistics on this measurement result. From the standard deviation statistical results, it can be seen that the timer measurement interval accuracy is 56.3 ps, and the SR540 measurement interval accuracy is 9.3 ps. It can be shown that the time interval timer can achieve a single measurement accuracy better than 60 ps, which has reached a relatively good level, but there is still a certain gap with SR540.

As shown in Figure 4, to evaluate the accuracy of the system measurement, in the actual test, the measurement value of the SR540 can be regarded as the true value based on the test method of the comparison method, and the value

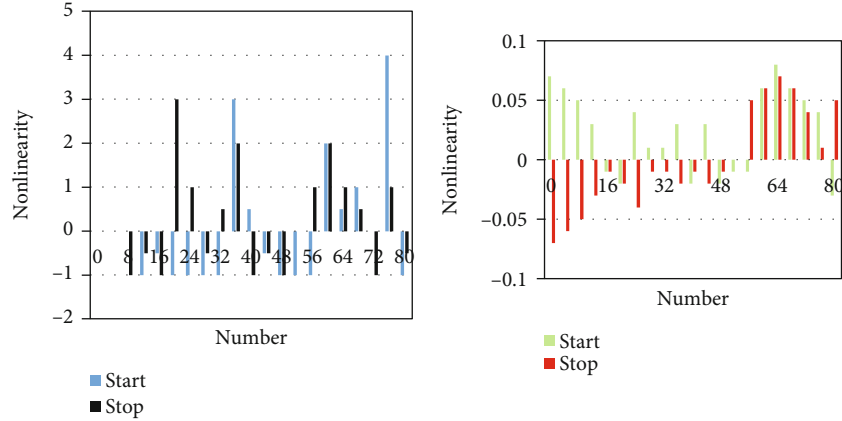


FIGURE 5: Start and stop differential integral nonlinear error results comparison.

TABLE 3: Simulation of the adjustment range of the oscillator.

VCTRL	26°C, 3 V		-50°C, 3 V	
	F	K	F	K
1	423		409	
1.2	463		432	
1.4	694		676	
1.6	789	649	767	752
1.8	892		865	
2	1100		1005	

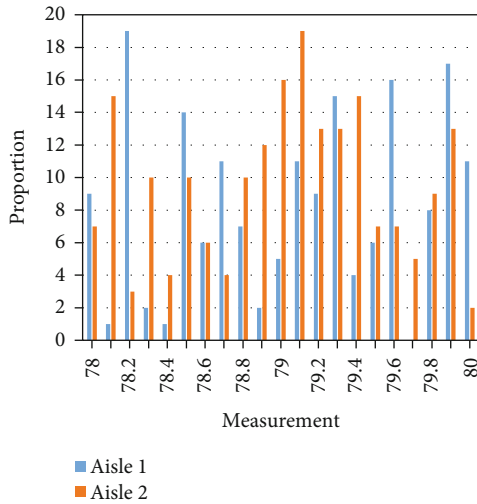


FIGURE 6: Probability distribution of measurement results.

measured by the timer and the SR540 synchronized measurement is subtracted. The difference between the two can be regarded as the accuracy of the system. It can be seen from the data that the accuracy test in two ways can ensure that the deviation of the system measurement is less than 495 ps.

4.2. Pulse Width Measurement Performance Test. In terms of measurement accuracy, the measurement result of this func-

tion is still compared with the pulse width measurement result of SR620. The pulse width to be measured is the 1 pps signal of the clock room of the National Time Service Center, and the reference clock is the 10 MHz signal of the clock room. This paper randomly selects 10 data for analysis, as shown in Table 2.

In Table 2, the error is controlled below 0.6, and the pulse width measurement range is around 204.85. Among them, the timer is not much different from the SR540, and the performance basically meets the standard requirements.

4.3. Differential and Integral Nonlinear Error Test. As shown in Figure 5, we can see the result of the differential nonlinearity error of a delay line (start), where the maximum value is 4 LSB and the minimum value is -1 LSB, where 1 LSB = 189.4 ps. It is the differential nonlinearity error of another delay line (stop), the maximum value is 3 LSB, the minimum value is -1 LSB, and 1 LSB = 173.6 ps. Start delay line's integral nonlinear error, the maximum value is 0.08 LSB, the minimum value is -0.03 LSB, and the average value of integral nonlinear error is 0.014 LSB, of which 1 LSB = 189.4 ps. The integral nonlinear error of the stop delay line, the maximum value is 0.07 LSB, the minimum value is -0.07 LSB, and the average value of integral nonlinear error is -0.03 LSB, where 1 LSB = 173.6 ps.

4.4. Oscillator Distribution Requirements. Changes in temperature and process will affect the frequency range of the output clock signal of the circuit. In order to ensure that the frequency of the output clock signal of the circuit can reach the design value, it is usually desirable to have the oscillator tuning range within the system frequency requirement range. The details are shown in Table 3.

When the temperature changes from low to high, the threshold voltage becomes smaller and K_{vco} decreases. The output frequency of the oscillator increases with the increase of its control voltage, which meets the theoretical requirements.

4.5. System Multichannel Measurement Conformance Test. This timer can measure multiple channels at the same time, so test the consistency of the measurement of different

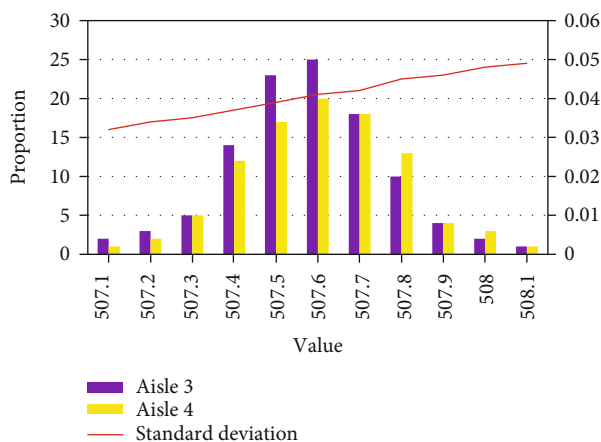


FIGURE 7: Multichannel measurement result distribution.

channels of the system. In this test, the second, third, and fourth channels are used to test the 100 m extension cable. Channel 2 is connected to the 1 pps signal output by the pulse distribution amplifier. Analyzing the multichannel calculation data, we get Figures 6 and 7.

It can be seen from Figure 6 that in a set of data, the fine measurement value and the final measurement result are normally distributed, indicating that the source of error in this measurement is mainly random error, but the single-channel fine measurement value is not very standardized. The normal distribution indicates that the measurement results are affected by errors other than random errors. But the final measured value still shows a more standardized normal distribution.

As shown in Figure 7, it can be seen from the statistical results of the standard deviation that the 3-channel measurement accuracy is 46.7 ps, and the 4-channel measurement accuracy is 33.2 ps. The measurement consistency of each channel is better, and the measurement accuracy is better than 50 ps. The results show a normal distribution, which further shows that the main source of noise that causes system measurement errors is random noise.

5. Conclusion

The ferroelectric memory is mainly composed of a data register, two counting units, and four output modules. The core of the device is a block circuit for timing, which includes a display, buttons, buzzer alarm indicator, and other components. During sports games, ferroelectric memory chips are used as carriers to transmit the sports event time information to the processor and save it. Then according to the program control the LED light to turn on or off the required sports data register to display the current time and start date, the end of the game, the results after the game, and the summary number after the game. Determine the size of each part and the connection relationship between each component according to the parameter values such as the movement time label and time as a reference basis. This article mainly uses the time interval measurement method and the experimental comparison method to study the equipment accu-

racy of the ferroelectric memory in the system in the sports timer. Through various experimental investigation results, it is concluded that the measurement uncertainty of the timer interval designed in this paper is better than 60 ps, the measurement data is accurate and reliable, and the signal pulse width measurement performance can be consistent with the international leading measurement equipment SR540. The timer in this article has certain fluctuations in the measurement result of the frequency signal, and its performance is not ideal. It needs to be processed by a suitable filtering algorithm to improve the frequency measurement accuracy of the timer.

Data Availability

No data were used to support this study.

Conflicts of Interest

The authors declare that there are no conflicts of interest regarding the publication of this article.

References

- [1] V. Jain, M. Swami, and R. Bansal, "Exploratory data analysis on username-password dataset," *Fusion: Practice and Applications*, vol. 4, no. 1, pp. 5–14, 2021.
- [2] M. Ismail, N. El-Rashidy, and N. Moustafa, "Mobile cloud database security: problems and solutions," *Fusion: Practice and Applications*, vol. 7, no. 1, pp. 15–29, 2021.
- [3] Q. Li, J. An'an, G. Hongxia et al., "Research on 60Co gamma rays and total electron dose effects of ferroelectric memory," *Acta Physica Sinica*, vol. 67, no. 16, pp. 272–279, 2018.
- [4] J. An'an, G. Hongxia, Z. Fengqi, G. Weixin, and O. Y. Xiaoping, "Experimental study on the single-event functional interruption effect induced by high-energy protons in ferroelectric memory," *Acta Physica Sinica*, vol. 67, no. 23, pp. 248–254, 2018.
- [5] F. Feizhuan, D. Jing, and L. Shuai, "Design of basketball match timing and coring device based on single chip computer," *Digital World*, vol. 169, no. 11, pp. 109–109, 2019.
- [6] Z. Pengcheng, "Design of 24-second countdown timer for basketball game based on AHDL language," *Electronic technology and software Engineering*, vol. 150, no. 4, pp. 81–82, 2019.
- [7] F. Kang, "The application of single-chip timer in timer design," *Fujian Computer*, vol. 35, no. 5, pp. 103–105, 2019.
- [8] F. Xiaocheng, L. Ping, and Z. Dehua, "Basketball timer experiment based on DE10_lite," *Journal of Electrical & Electronic Education*, vol. 42, no. 3, pp. 125–128, 2020.
- [9] W. Zhiming, "Elementary school science based on concept transformation strategy exploration-record of the demonstration lesson of "making a one-minute timer"," *Teaching Management and Education Research*, vol. 3, no. 10, pp. 72–77, 2018.
- [10] J. Wei, "The production of countdown timer based on action script," *Computer Knowledge and Technology*, vol. 13, no. 16, pp. 185–186, 2017.
- [11] T. Zerong, "Analysis of MCS-51 single-chip stopwatch design," *Success: Education*, no. 16, pp. 35–37, 2017.

- [12] Z. Chao, W. Miao, and Z. Hongxin, "Design and simulation analysis of digital circuit "stopwatch" based on Proteus," *Electronic Design Engineering*, vol. 28, no. 10, pp. 46–50, 2020.
- [13] V. K. Rishu and S. A. Sinha, "Advancements in encryption techniques for enhanced data security over cloud," *Journal of Cybersecurity and Information Management*, vol. 8, no. 2, pp. 51–59, 2021.
- [14] D. Shihua and S. Zubin, "Design and implementation of high-precision electronic stopwatch based on EDA technology," *Science and Technology Innovation and Application*, vol. 275, no. 19, pp. 98–99, 2019.
- [15] Q. Believes, C. Yiguang, T. Enling, and H. Yafei, "Damage effect and thermal evolution induced by femtosecond pulsed laser irradiation FRAM," *Acta Luminescence*, vol. 40, no. 6, pp. 815–825, 2019.
- [16] T. Pengfei, L. Bo, W. Jinbin, Z. Xiangli, G. Hongxia, and W. Fang, "Simulation of the effect of ionizing radiation on the domain structure of ferroelectric thin films," *Natural Science Journal of Xiangtan University*, vol. 41, no. 4, pp. 30–39, 2019.
- [17] C. Linggang, C. Hongyue, D. Zhihong, and Z. Ximan, "Application research of ferroelectric memory in strapdown inertial navigation system," *China Equipment Engineering*, no. 11, pp. 184–185, 2019.
- [18] L. Shuang, Z. Yinlian, T. Yunlong, Z. Sirui, M. Jinyuan, and M. Xiuliang, "Evolution of ferroelectric vortex structure in superlattice," *Chinese Journal of Chinese Electron Microscopy Society*, vol. 37, no. 4, pp. 14–18, 2018.
- [19] W. Pengbo, "Fault model of ferroelectric memory and march C-1T1C test," *Henan Science and Technology*, vol. 39, no. 28, pp. 9–12, 2020.
- [20] Y. Dina, "The MSP430 family adds an intelligent analog combination to make the MCU flexible and configurable," *Microcontrollers and Embedded System Applications*, vol. 18, no. 7, pp. 99–99, 2018.
- [21] S. Shiyu, S. Hongjia, Z. Xiangli, Z. Yi, and W. Jinbin, "Research on the storage characteristics and reliability of metal-ferroelectric layer (BNT)-insulating layer (YSZ)-semiconductor (Si) diodes," *Modern Applied Physics*, vol. 8, no. 2, pp. 62–66, 2017.
- [22] W. Peng, W. Shansheng, W. Min, S. Zhimin, and H. Rui, "Research on water temperature measurement device for intelligent drilling wells," *Electronics World*, vol. 15, pp. 40–42, 2019.
- [23] Y. Qiao, L. Xiaochi, and C. Mingchao, "Research progress in preparation technology of barium strontium titanate nanopowders," *Chinese Ceramics*, vol. 53, no. 1, pp. 9–14, 2017.